DEPARTMENT OF AEROSPACE ENGINEERING

GSC'25 Conference
July 14, 2025

FMLAB

Stability Analysis of Shear Flows Utilizing the Small-Gain Theorem

Ofek Frank-Shapir, Igal Gluzman
Fluid Mechanics Laboratory
Faculty of Aerospace Engineering, Technion

Flow Stability

- Stability analysis is used in the context of fluid dynamics to assess at what conditions a **laminar** flow becomes **turbulent**
- **Laminar flow** - smooth orderly flow that moves in parallel layers (laminae) with no unsteady macroscopic mixing or overturning motion of the layers.
- **Turbulent flow** - irregular disorderly flow with unsteady, chaotic three-dimensional macroscopic mixing motions.
- **Flow instability** may be triggered by disturbance, and **transition from laminar to turbulent flow** state may occur.
- Key parameter in studying flow stability is the **Reynolds number** (Re) - dimensionless quantity measuring the ratio between inertial and viscous forces.

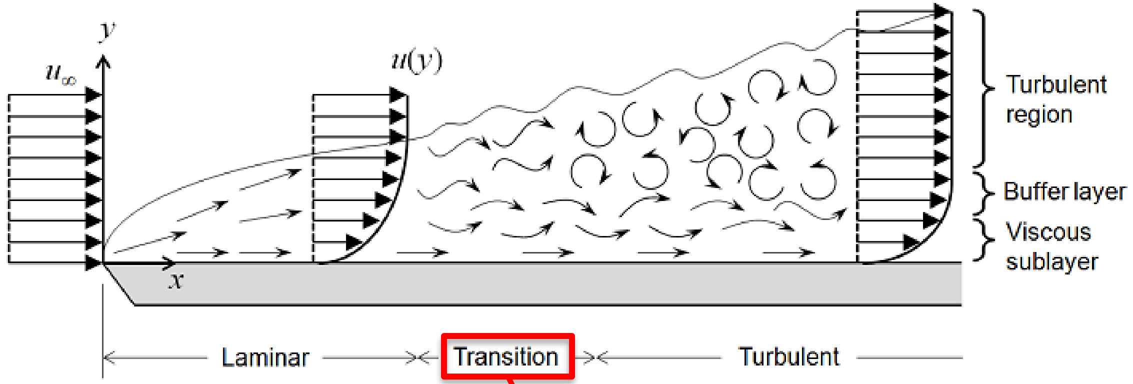

Image source:su2code.github.io

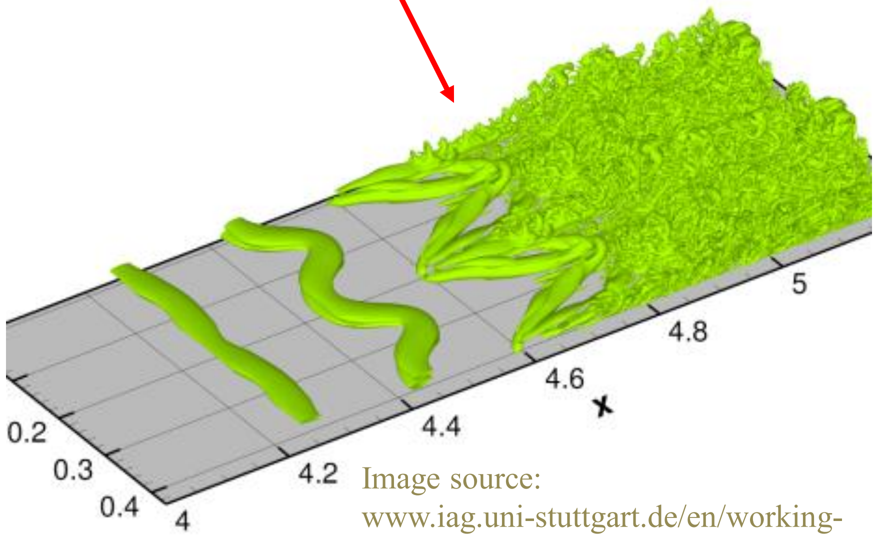

Image source: www.iag.uni-stuttgart.de/en/working-groups/transition-and-turbulence

Background

- Two main approaches are used in transition studies:
  - Modal analysis – e.g., hydrodynamic linear stability theory (LST)
    - Eigenvalue analysis of the flow response to initial conditions
    - Infinitesimal disturbances superimposed on a base flow
    - Defined in the infinite horizon sense, while short-time perturbation dynamics are disregarded (Schmid 2007).
  - Nonmodal analysis – e.g., transient growth, input-output analysis
    - Allows detailed analysis of the response to external forcing (e.g., input-output formulation that contains a transfer function)
    - Allows studying flow behavior in the finite horizon sense (e.g., transient growth due to the non-normality of the LNS operator)

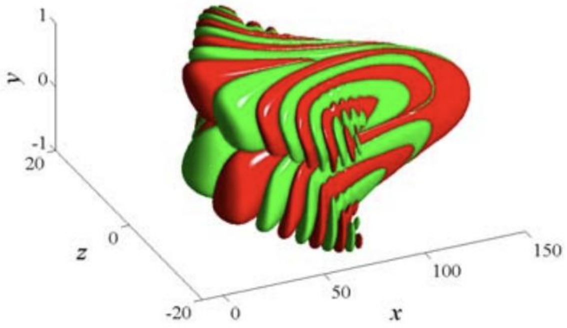

Reprinted from Fig. 10.6, Jovanovic, Thesis, 2004

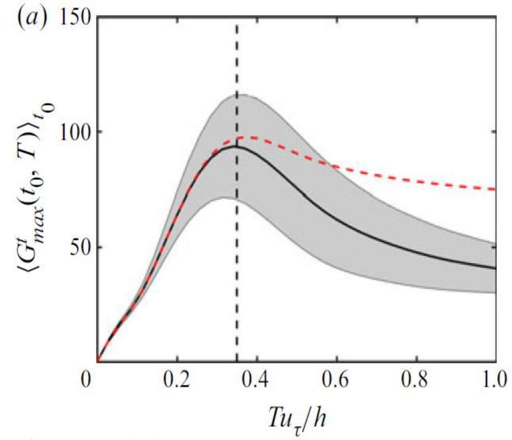

Reprinted from Fig. 11(a), A. Lozano-Durán et al., JFM, 2020

Motivation – Critical Reynolds Number

- LST predicts Couette flow to be stable at all Reynolds numbers
  - Experiments (Tillmark & Alfredsson 1992; Dauchot & Daviaud 1995) and simulation results (Dou & Khoo 2012; Barkley & Tuckerman 2005) show transition at $Re = 320 - 370$
- LST predicts transition of Poiseuille flow at $Re = 5772$
  - Experimental results (Sano & Tamai 2016) show transition at Reynolds numbers as low as $Re = 842$

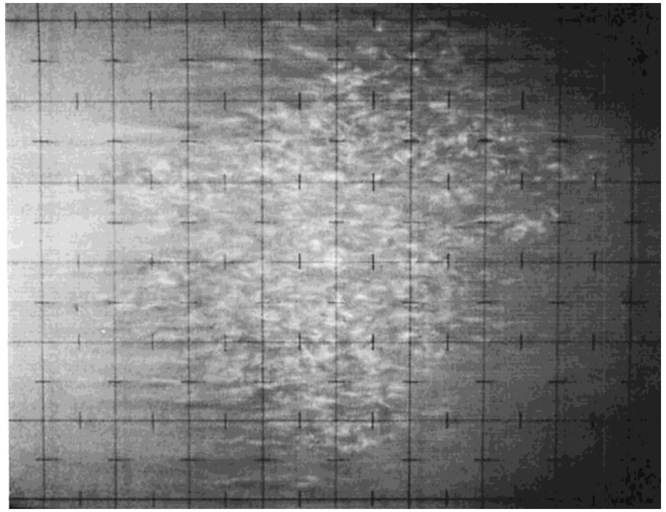

Reprinted from Fig. 6, Tillmark & Alfredsson, Eur. J. Mech 1992

Turbulent spot in plane Couette flow for $Re = 405$

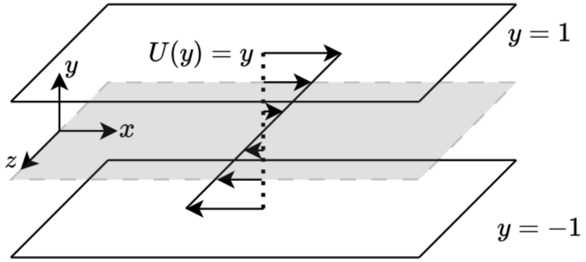

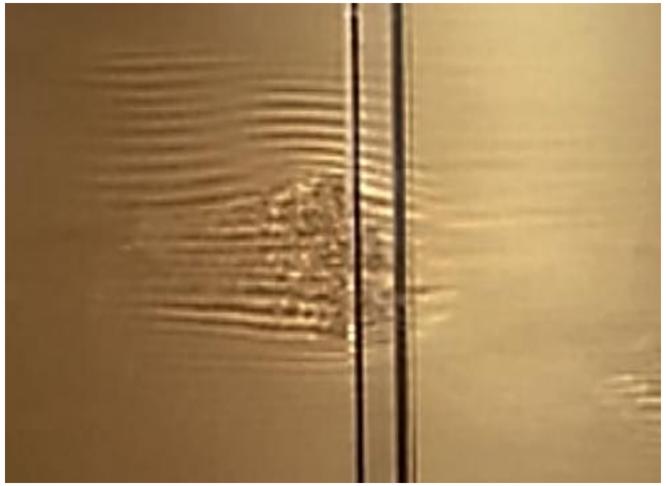

Reprinted from Fig. 1, Sano & Tamai, Nature physics, 2016

Turbulent spot surrounded by laminar flow in plane Poiseuille flow for $Re = 842$

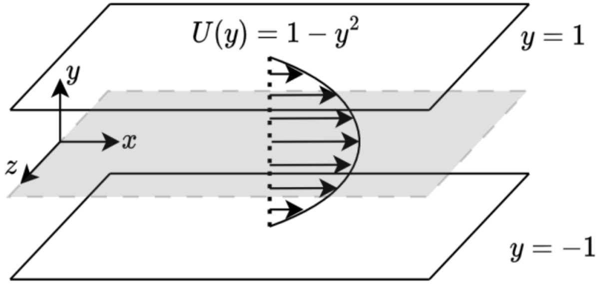

Motivation – Effect of Perturbation Magnitude

- Experiments also show that flow can remain stable for larger Reynolds number than the critical value predicted by LST (up to $Re = 100{,}000$ for pipe flow) by reducing disturbance magnitude (Pfenniger 1961; Avila et al. 2023)

Disturbance magnitude has an impact on the stability of flows. This motivates us to focus on developing a stability criterion that accounts for **finite disturbance magnitude**.

Outline

- Mathematical Background
  - Navier-Stokes equations for perturbations
  - Input-output analysis
  - Small gain theorem utilization for flow stability analysis

- Unstructured Nonlinearity
  - Stability analysis for 2D modes

- Structured Nonlinearity
  - Modeling nonlinearity structure using SSVs
  - Stability analysis for 2D modes
  - Stability analysis for 3D modes

Linear Input-Output Analysis

- Linearized Navier-Stokes equation for perturbations:

$$\partial_t \boldsymbol{u} = -U \cdot \nabla \boldsymbol{u} - \boldsymbol{u} \cdot \nabla \mathrm{U} - \nabla p + \frac{1}{Re} \nabla^2 \boldsymbol{u} + \boldsymbol{f}$$

Farrell & Ioannou (93 PF); Bamieh & Dahleh (01 PF); Jovanović & Bamieh (01 ACC,05 JFM); Bagheri et al. (09 JFM); McKeon & Sharma (10 JFM); Hariharan et al. (18 JNNFM);

Fourier transform in x, z directions and in time; $(x, z, t) \rightarrow (k_x, k_z, \omega)$

$$\begin{matrix} \dot{\psi} = A\psi + Bf \\ \phi(\omega, k_x, y, k_z) = C\psi \end{matrix}, \text{where } \psi = \begin{bmatrix} v \\ \omega_y \end{bmatrix}, \phi = \begin{bmatrix} u \\ v \\ w \end{bmatrix}$$

- Input – forcing
- Output – velocity perturbations vector
- Frequency response operator:
  $\mathcal{H}(y; k_x, k_z, \omega) = C(i\omega I - A)^{-1}B$

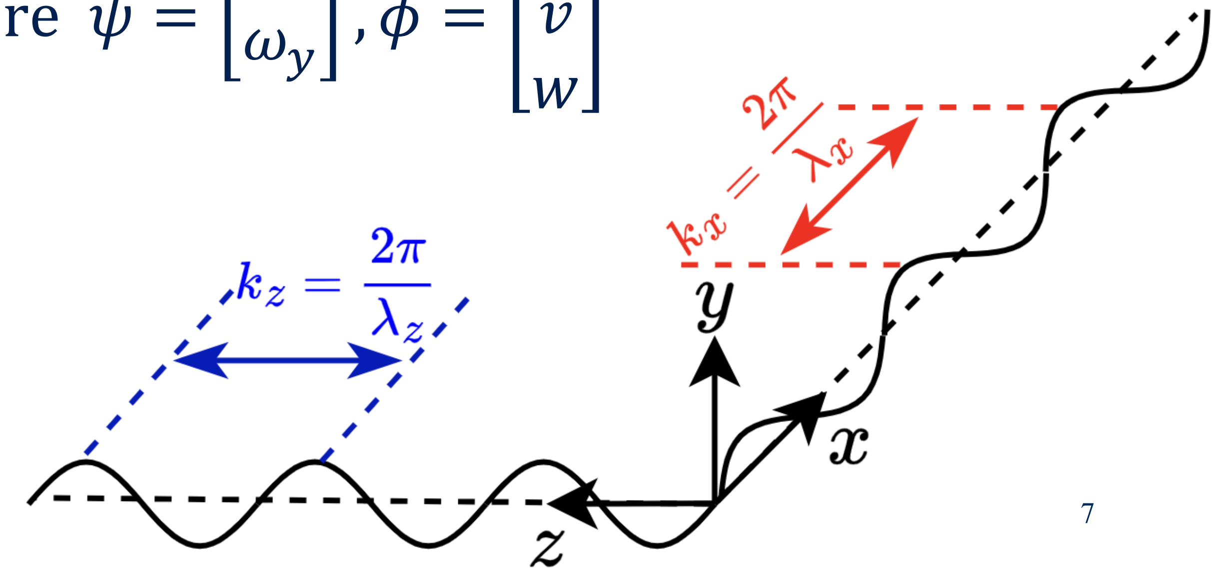

Structured Input-Output Analysis formulation

- Navier-Stokes equation for perturbations (no forcing):

$$\partial_t \boldsymbol{u} = -U \cdot \nabla \boldsymbol{u} - \boldsymbol{u} \cdot \nabla \mathrm{U} - \nabla p + \frac{1}{Re}\nabla^2 \boldsymbol{u} - \boldsymbol{u} \cdot \nabla \boldsymbol{u}$$

- Use nonlinear term ($\boldsymbol{u} \cdot \nabla \boldsymbol{u}$) as a feedback forcing term (Liu and Gayme, 2021)
- $\mathbf{u}_{\Xi}$ - matrix gain that results in the structure of the nonlinear term

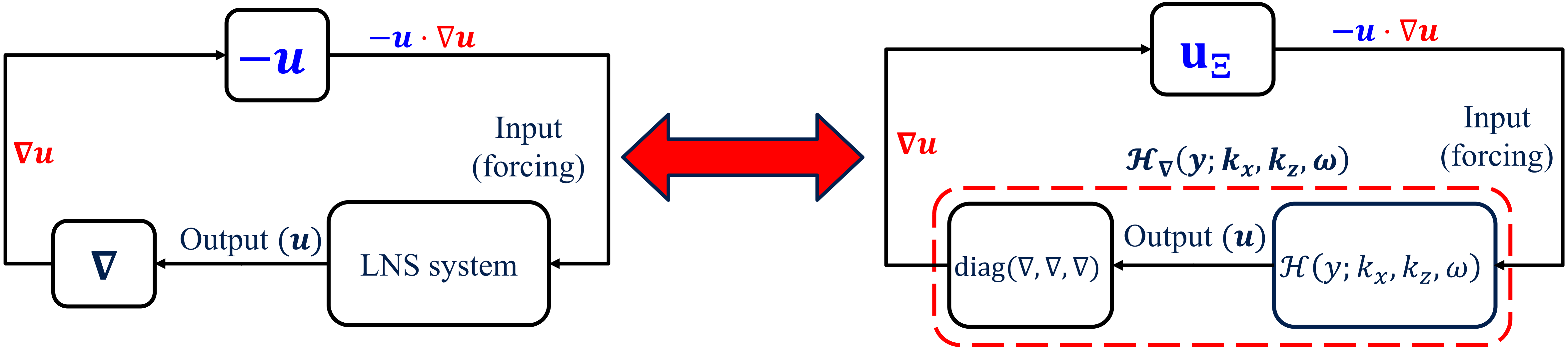

- We combine the gradient operator with $\mathcal{H}$ to obtain operator $\mathcal{H}_{\nabla}$ (forcing→velocity perturbation derivatives)

Choice of Norms

- Amplification of kinetic energy density:

$$\|\mathcal{H}\|_2^2(k_x,k_z) = \frac{1}{2\pi}\int_{-\infty}^{\infty} \mathrm{trace}[\mathcal{H}(y;k_x,k_z,\omega)\mathcal{H}^*(y;k_x,k_z,\omega)]d\omega$$

- Amplification of most amplified velocity eigenvector:

$$\|\mathcal{H}\|_\infty(k_x,k_z) = \sup_{\omega\in\mathbb{R}} \bar{\sigma}[\mathcal{H}(y;k_x,k_z,\omega)],$$

$\bar{\sigma}$ - largest singular value

- $\|\cdot\|_\infty$ represents the "worst case" amplification and is thus suited for formulating a stability criterion

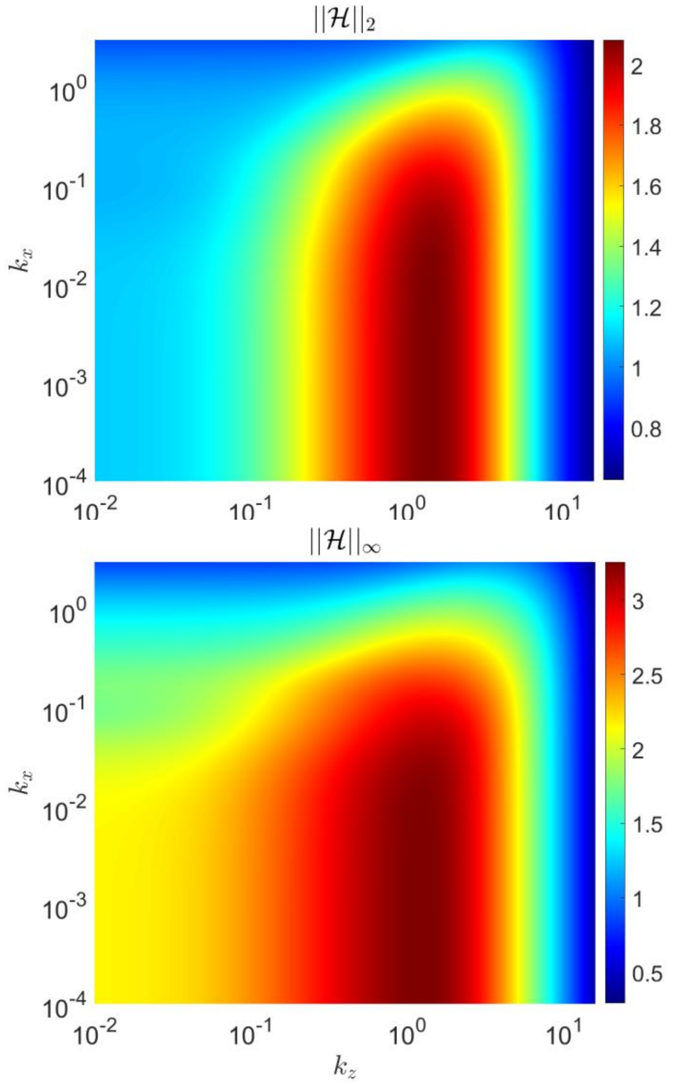

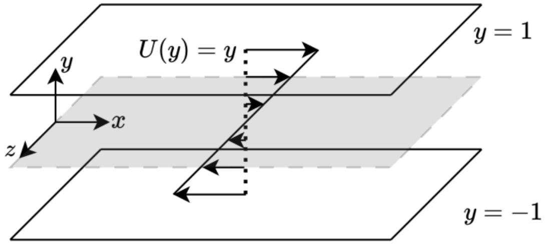

$$Re = \frac{hU}{\nu} = 300$$

Stability Analysis via Small Gain Theorem

- We use the small gain theorem to derive a **stability criterion** for shear flows that accounts for **finite disturbance magnitude**

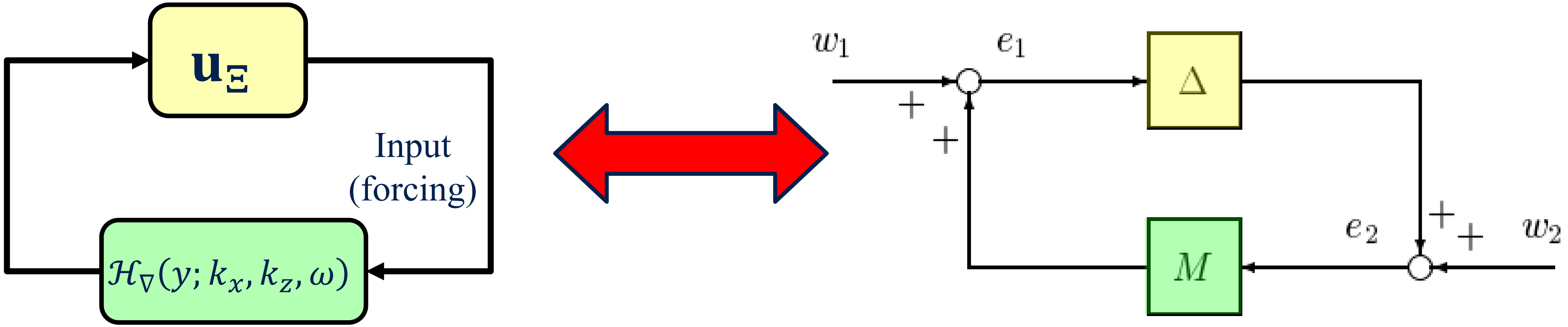

Reprinted from Robust and optimal control, Zhou et al.,1995.

Theorem 9.1 (Small Gain Theorem) *Suppose* $M \in \mathcal{RH}_\infty$. *Then the interconnected system shown in Figure 9.3 is well-posed and internally stable for all* $\Delta(s) \in \mathcal{RH}_\infty$ *with*

(a) $\|\Delta\|_\infty \leq 1/\gamma$ *if and only if* $\|M(s)\|_\infty < \gamma$;

(b) $\|\Delta\|_\infty < 1/\gamma$ *if and only if* $\|M(s)\|_\infty \leq \gamma$.

Stability Analysis via Small Gain Theorem

- In our case:

$$\|\mathbf{u}_\Xi\|_\infty = \sup_{y\in\mathcal{Y}}[\bar{\sigma}(\mathbf{u}_\Xi)] = \sup_{y\in\mathcal{Y}}\|\boldsymbol{u}(y)\|_2 \Leftrightarrow \text{maximal disturbance}, u_{\max}$$

Where $\mathcal{Y} = [-1,1]$ for channel flows and $\mathcal{Y} = [0,\infty)$ for boundary layers

- Requirement for stability utilizing the small gain theorem:

$$\sup_{y\in\mathcal{Y}}\|\boldsymbol{u}(y)\|_2 < 1/\gamma \Leftrightarrow \|\mathcal{H}_\nabla\|_\infty \leq \gamma$$

$$\Downarrow$$

$$\sup_{y\in\mathcal{Y}}\|\boldsymbol{u}(y)\|_2 \leq \|\mathcal{H}_\nabla\|_\infty^{-1}$$

- Bound on **velocity perturbation magnitude** that ensures stability of the system:

$$u_{\max} \leq \|\mathcal{H}_\nabla\|_\infty^{-1}$$

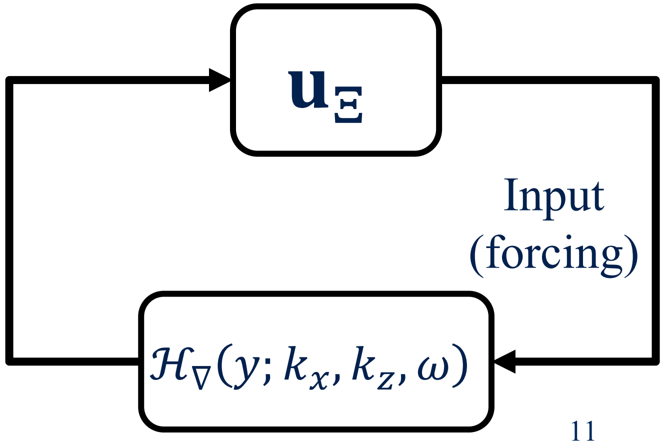

Stability for 2D modes

- Couette base flow
- Only 2D modes are considered ($k_z = 0$)
- Stability for selected perturbations of amplitude $||\boldsymbol{u}||_2 = 10^{-2.4}$
- $Re_{cr} = 320$ matches experimental results (Tillmark & Alfredsson 1992; Dauchot & Daviaud 1995)
- This analysis can be extended to any perturbation magnitude

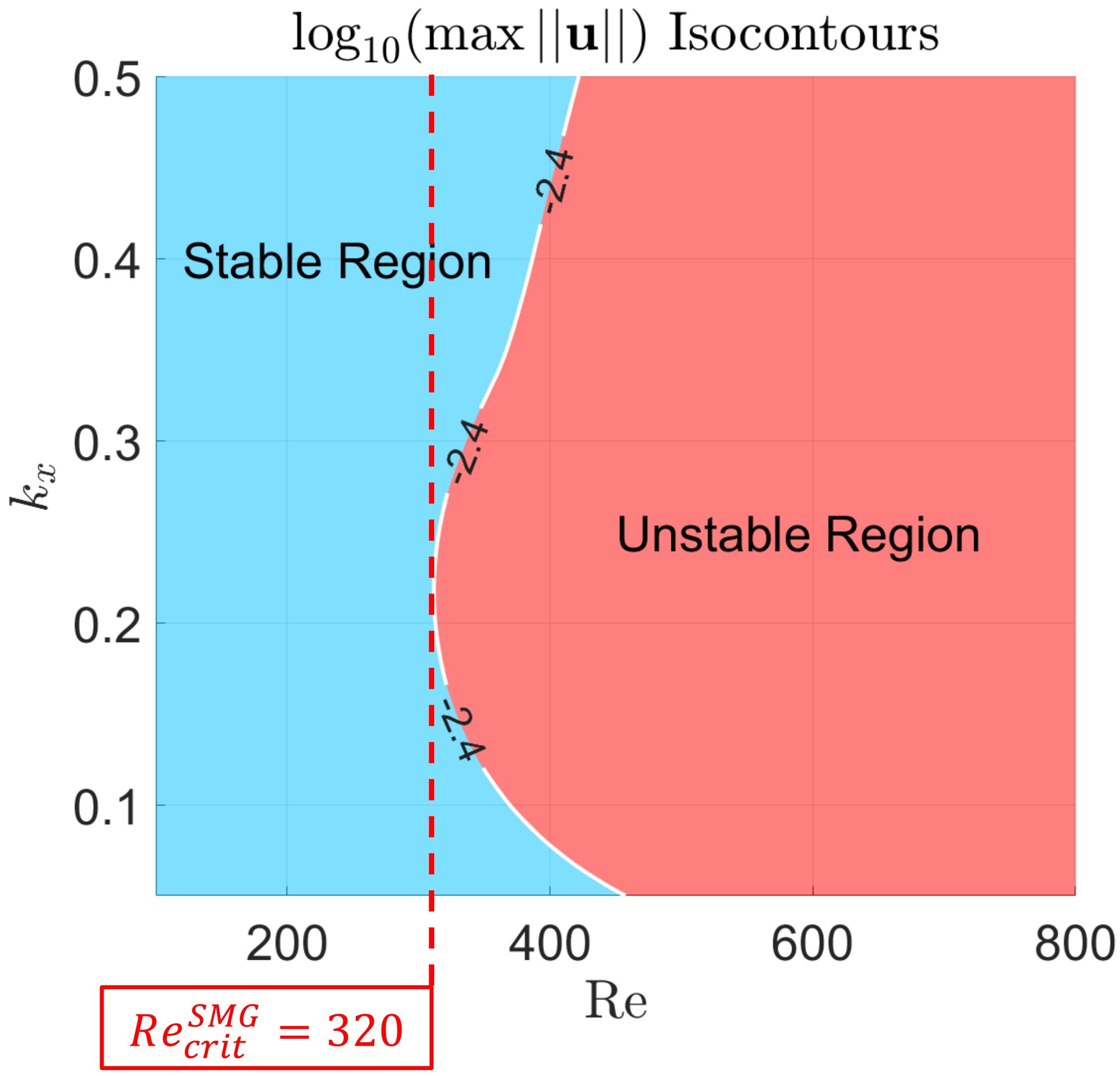

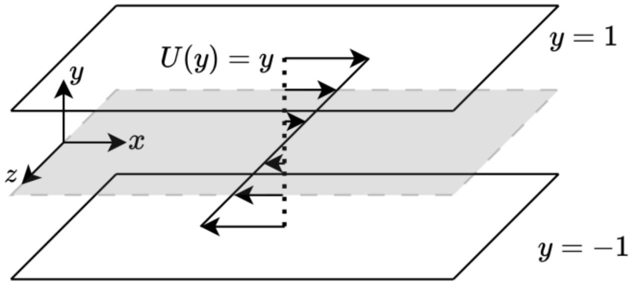

Stability for 2D modes ($k_z = 0$)

Couette flow

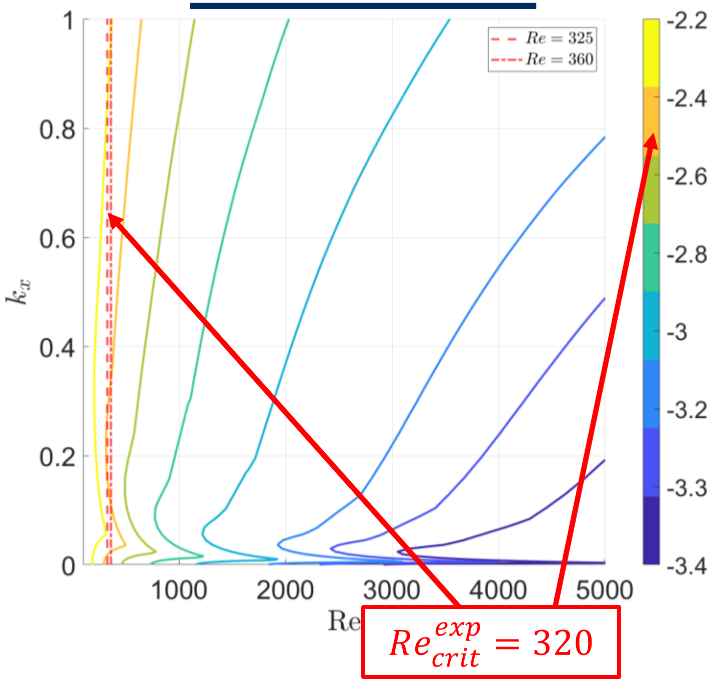

Poiseuille flow

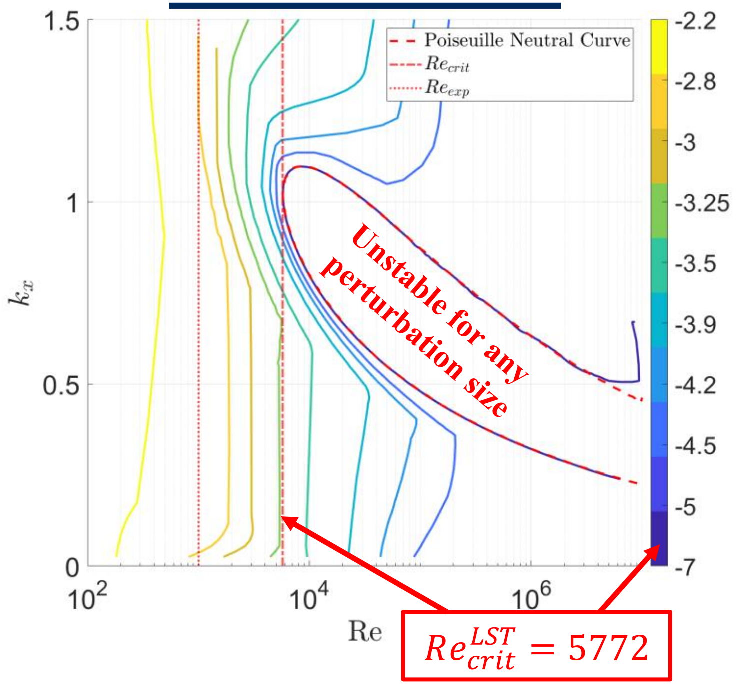

Blasius flow

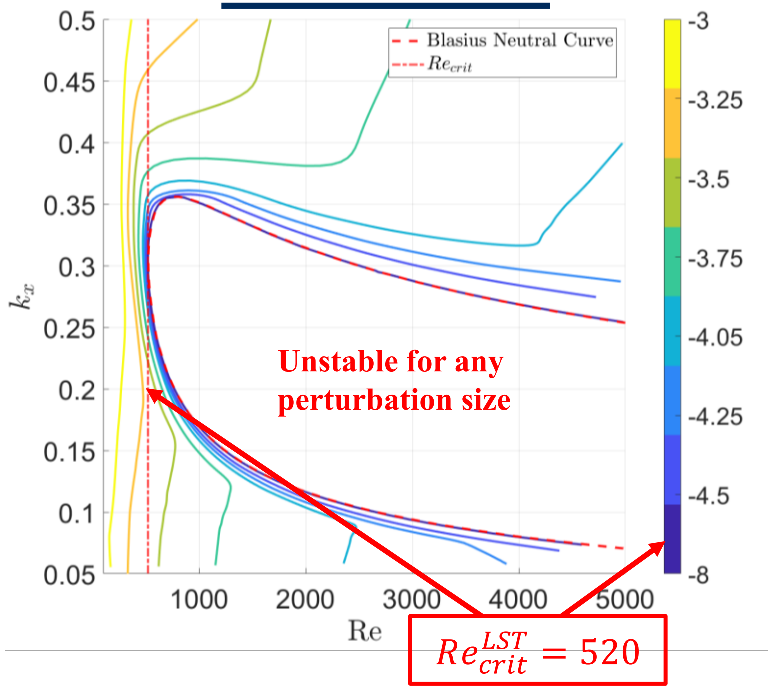

- Given large enough perturbation magnitude – the flow can become unstable
- As the Reynolds number increases – smaller perturbations cause instability

For infinitesimally small disturbance ($\|\boldsymbol{u}\|_2$) – results approach LST
As perturbation size increases – the critical Reynolds number decreases

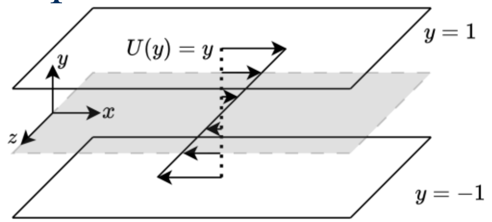

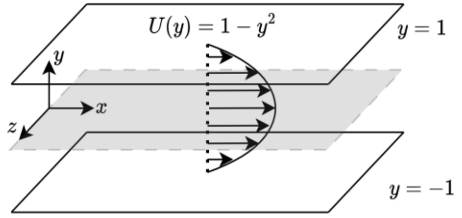

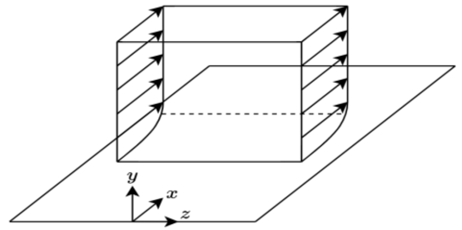

Structured Input-Output Analysis

- Response is quantified by computing structured singular values (SSVs) of $\mathcal{H}_\nabla$ (Packard & Doyle 1993)

- **SSVs** - obtained by solving the minimization problem:

$$\mu_{\boldsymbol{\Delta}_\mathbf{u}}(\mathcal{H}_\nabla) = \frac{1}{\min\{\bar{\sigma}(\mathbf{u}_\Xi)\ :\ \det(I - \mathcal{H}_\nabla \mathbf{u}_\Xi) = 0,\ \ \mathbf{u}_\Xi \in \boldsymbol{\Delta}_\mathbf{u}\}},$$

$$\|\mathcal{H}_\nabla\|_{\mu_{\boldsymbol{\Delta}_\mathbf{u}}} = \sup_{\omega \in \mathbb{R}} \left[\mu_{\boldsymbol{\Delta}_\mathbf{u}}(\mathcal{H}_\nabla)\right]$$

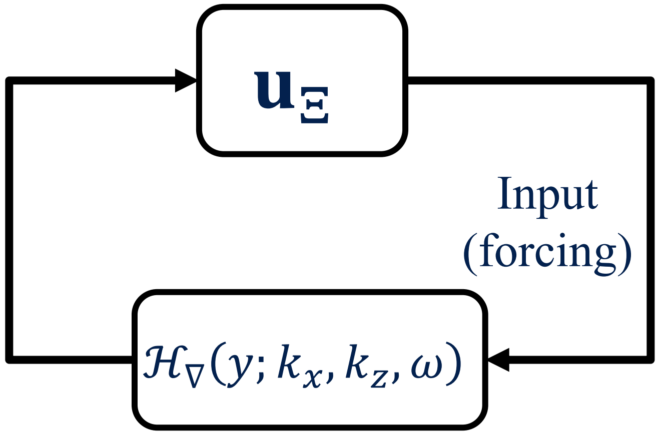

$\mathbf{u}_\Xi$ – Interconnected uncertainty

$\boldsymbol{\Delta}_\mathbf{u}$ – The structure of the interconnected uncertainty

$\mu_{\Delta_\mathbf{u}}(\cdot)$ – the largest SSV with respect to a structure $\Delta_\mathbf{u}$

$\bar{\sigma}(\cdot)$ – largest singular value

$\det(\cdot)$ – determinant operation

Structure of Uncertainty

- $\boldsymbol{\Delta}_{\mathbf{u}} = \{\mathbf{u}_{\Xi} = \mathbf{I}_{3\times3} \otimes \Delta_u, \Delta_u = \left[\text{diag}(u_\xi), \text{diag}(v_\xi), \text{diag}(w_\xi)\right]: \text{u}_\xi, v_\xi, w_\xi \in \mathbb{C}^{N_y \times 1}\}$

- $\boldsymbol{\Delta}_{\mathbf{u}}$ - uncertainty structure that matches the structure of $\mathbf{u}_{\Xi}$

- $\mathbf{u}_{\Xi}$ - diagonal block matrix with repeating blocks, where the blocks have 3 diagonals

- Computing SSVs under $\boldsymbol{\Delta}_{\mathbf{u}}$ requires complex set of constraints to preserve the structure of $\mathbf{u}_{\Xi}$

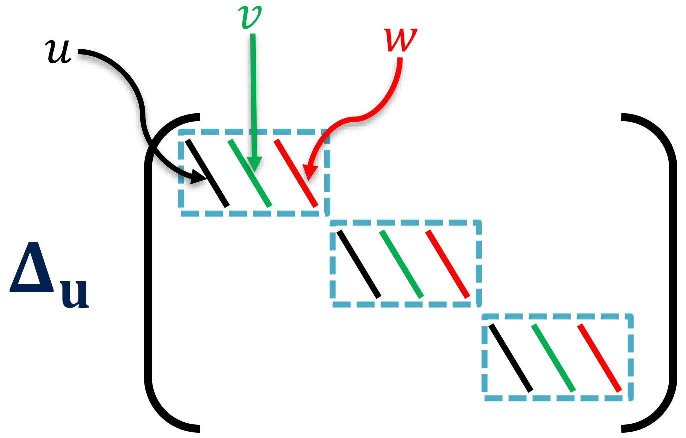

Such a solution has not yet been found

Approximating the structure of $\mathbf{\Delta_u}$

- Repeated full – block matrix (Mushtaq, et al., 2024)

$$\mathbf{\Delta}_r = \{\mathbf{I}_{3\times 3} \otimes \Delta_r : \Delta_r \in \mathbb{C}^{3N_y \times N_y}\}$$

$\mathbf{\Delta}_r$

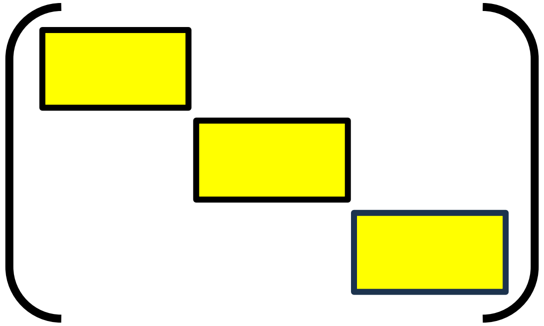

- Full – block matrix with different blocks (Liu and Gayme, 2021)

$$\mathbf{\Delta}_{nr} = \{\mathrm{diag}(\Delta_1, \Delta_2, \Delta_3) : \Delta_i \in \mathbb{C}^{3N_y \times N_y}, i \in \{1,2,3\}\}$$

$\mathbf{\Delta}_{nr}$

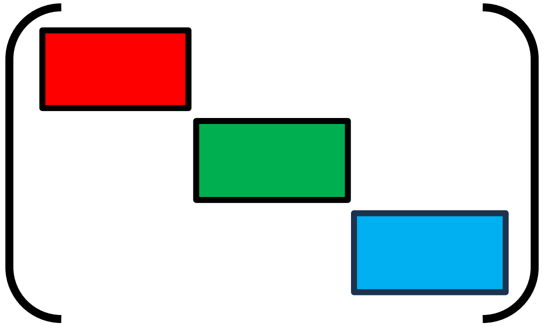

Structured Stability Analysis

- Our stability criterion based on the small gain theorem can be updated to account for the structure of the nonlinear term
- **Structured analysis:**
  - Accurate structure: $$u_{\max} \leq \|\mathcal{H}_\nabla\|^{-1}_{\mu_{\mathbf{\Delta_u}}}(k_x, k_z)$$

$\mathbf{\Delta_u}$ 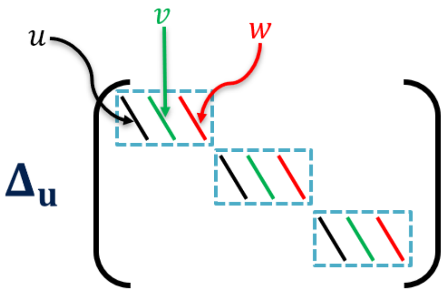

  - Approximated structures: $$u_{\max} \leq \|\mathcal{H}_\nabla\|^{-1}_{\mu_{\mathbf{\Delta}_r}}(k_x, k_z)$$

$\mathbf{\Delta}_r$ 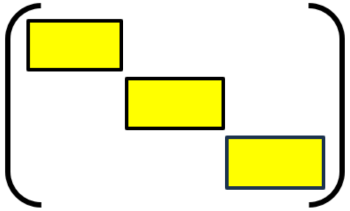

$$u_{\max} \leq \|\mathcal{H}_\nabla\|^{-1}_{\mu_{\mathbf{\Delta}_{nr}}}(k_x, k_z)$$

$\mathbf{\Delta}_{nr}$ 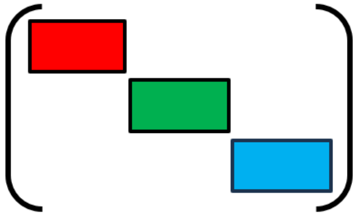

- **Unstructured analysis:**

$$u_{\max} \leq \|\mathcal{H}_\nabla\|^{-1}_{\infty}(k_x, k_z)$$

Structure Effect on Stability

- Blasius flow, $(\mathrm{Re} - k_x)$ maps for $k_z = 0$:

Unstructured:

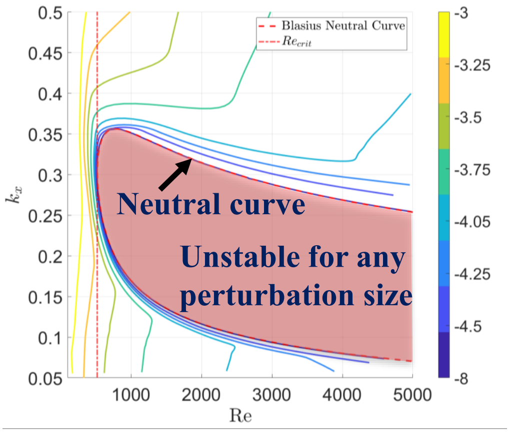

Non-repeated:

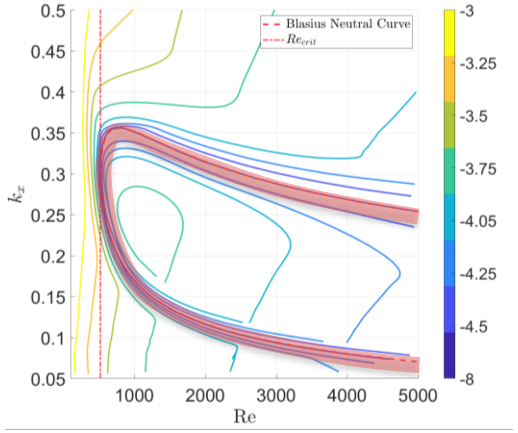

- Outside the neutral curve region, similar behavior between structured and unstructured cases
- Imposing structure shows that the least stable region is confined to a neutral curve envelope.

- Blasius flow, $(k_z - k_x)$ maps for $Re = 400$:

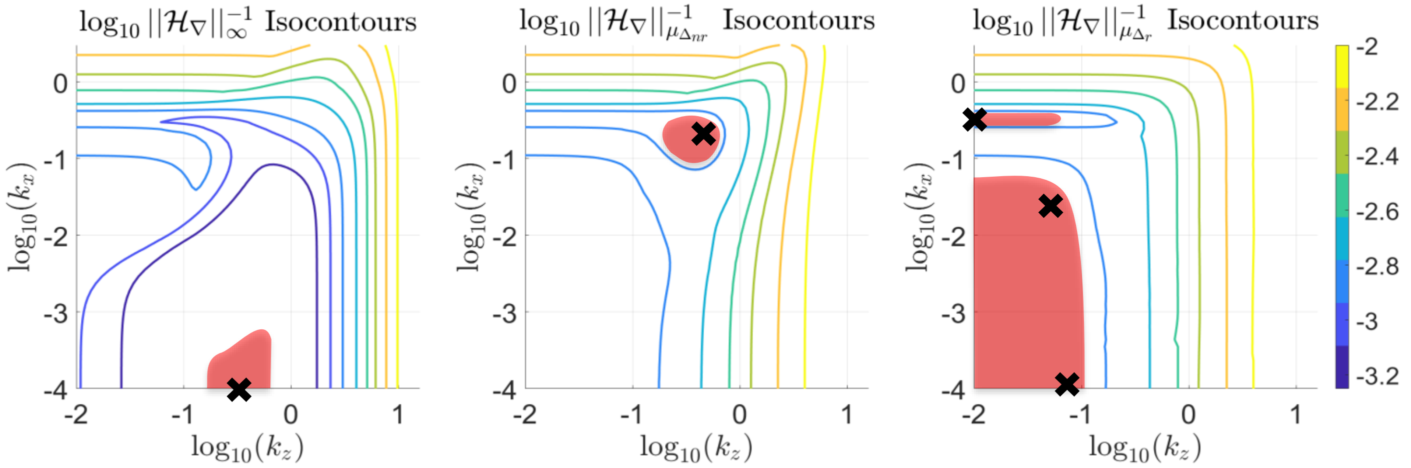

- Least stable modes:

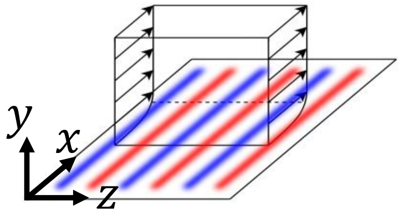

Streaky structures

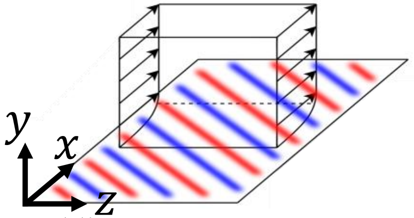

Oblique waves

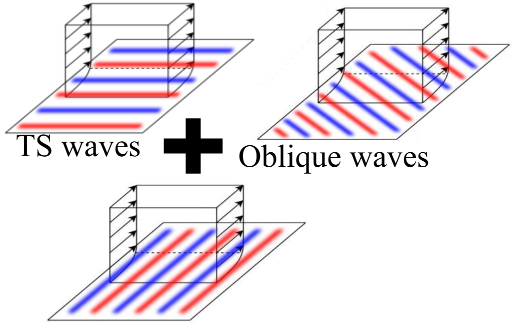

Streaky structures

- The spatial shape of the least stable mode depends on the structure of the nonlinearity
- For the case of repeated blocks –a wide range of dominant unstable modes is possible.

Conclusions

- We derived a stability criterion to analyze shear flows and boundary layers based on disturbance magnitude, utilizing the **small gain theorem.**
  - **Converges to LST predictions of critical Reynolds number** for infinitesimal disturbances
  - **Expands on linear stability theory (LST)** by allowing for finite-amplitude perturbations

- **Predicts instability of Couette flow** as observed in experiments in contrast to LST predictions
- Shows that flow can become unstable for a wide range of Reynolds numbers, **depending on the magnitude of perturbations** present in the flow

- Can be modified to include constraints on the structure of the nonlinearity using **structured singular values**
- Streaky structures, which are shown to be dominant in unstructured I/O approach, lose their dominance when using structured I/O approaches.

- Our approach allows to analyze flow stability in **noisy environments,** such as in real-life applications and wind tunnel experiments**, and explore bypass transition scenarios.**

Thank You!

Backup slides

Linear State-Space

$$\mathscr{A} \equiv \begin{bmatrix} \mathscr{A}_{11} & 0 \\ \mathscr{A}_{21} & \mathscr{A}_{22} \end{bmatrix} \equiv \begin{bmatrix} -ik_x\Delta^{-1}U\Delta + ik_x\Delta^{-1}U'' + \frac{1}{Re}\Delta^{-1}\Delta^2 & 0 \\ -ik_zU' & -ik_xU + \frac{1}{Re}\Delta \end{bmatrix},$$

$$\mathscr{B} \equiv \begin{bmatrix} \mathscr{B}_x & \mathscr{B}_y & \mathscr{B}_z \end{bmatrix} \equiv \begin{bmatrix} \Delta^{-1} & 0 \\ 0 & I \end{bmatrix} \begin{bmatrix} -ik_x\frac{\partial}{\partial y} & -(k_x^2+k_z^2) & -ik_z\frac{\partial}{\partial y} \\ ik_z & 0 & -ik_x \end{bmatrix},$$

$$\mathscr{C} \equiv \begin{bmatrix} \mathscr{C}_u \\ \mathscr{C}_v \\ \mathscr{C}_w \end{bmatrix} \equiv \frac{1}{k_x^2+k_z^2} \begin{bmatrix} ik_x\frac{\partial}{\partial y} & -ik_z \\ k_x^2+k_z^2 & 0 \\ ik_z\frac{\partial}{\partial y} & ik_x \end{bmatrix}.$$

$$\mathscr{H}(k_x,k_z,\omega) = \mathscr{C}(k_x,k_z)(i\omega I - \mathscr{A}(k_x,k_z))^{-1}\mathscr{B}(k_x,k_z).$$

$$\|\mathscr{H}(k_x,k_z,\omega)\|_2^2 \equiv \frac{1}{2\pi}\int_{-\infty}^{\infty} \mathrm{trace}[\mathscr{H}(k_x,k_z,\omega)\mathscr{H}^*(k_x,k_z,\omega)]d\omega.$$

$\mathcal{H}$ Operator Components

$$\mathscr{H}(k_x,k_z,\omega)=\begin{bmatrix}\mathscr{C}_u\\ \mathscr{C}_v\\ \mathscr{C}_w\end{bmatrix}(i\omega I-\mathscr{A}(k_x,k_z))^{-1}\begin{bmatrix}\mathscr{B}_x & \mathscr{B}_y & \mathscr{B}_z\end{bmatrix}\equiv$$

$$\equiv\begin{bmatrix}\mathscr{H}_{ux}(k_x,k_z,\omega) & \mathscr{H}_{uy}(k_x,k_z,\omega) & \mathscr{H}_{uz}(k_x,k_z,\omega)\\ \mathscr{H}_{vx}(k_x,k_z,\omega) & \mathscr{H}_{vy}(k_x,k_z,\omega) & \mathscr{H}_{vz}(k_x,k_z,\omega)\\ \mathscr{H}_{wx}(k_x,k_z,\omega) & \mathscr{H}_{wy}(k_x,k_z,\omega) & \mathscr{H}_{wz}(k_x,k_z,\omega)\end{bmatrix}.$$

$$\mathscr{H}(k_x,k_z,\omega)=\mathscr{C}(i\omega I-\mathscr{A}(k_x,k_z))^{-1}\begin{bmatrix}\mathscr{B}_x & \mathscr{B}_y & \mathscr{B}_z\end{bmatrix}\equiv$$

$$\equiv\begin{bmatrix}\mathscr{H}_x(k_x,k_z,\omega) & \mathscr{H}_y(k_x,k_z,\omega) & \mathscr{H}_z(k_x,k_z,\omega)\end{bmatrix},$$

$$\mathscr{H}(k_x,k_z,\omega)=\begin{bmatrix}\mathscr{C}_u\\ \mathscr{C}_v\\ \mathscr{C}_w\end{bmatrix}(i\omega I-\mathscr{A}(k_x,k_z))^{-1}\mathscr{B}\equiv$$

$$\equiv\begin{bmatrix}\mathscr{H}_u(k_x,k_z,\omega)\\ \mathscr{H}_v(k_x,k_z,\omega)\\ \mathscr{H}_w(k_x,k_z,\omega)\end{bmatrix}.$$

Eigenvalues

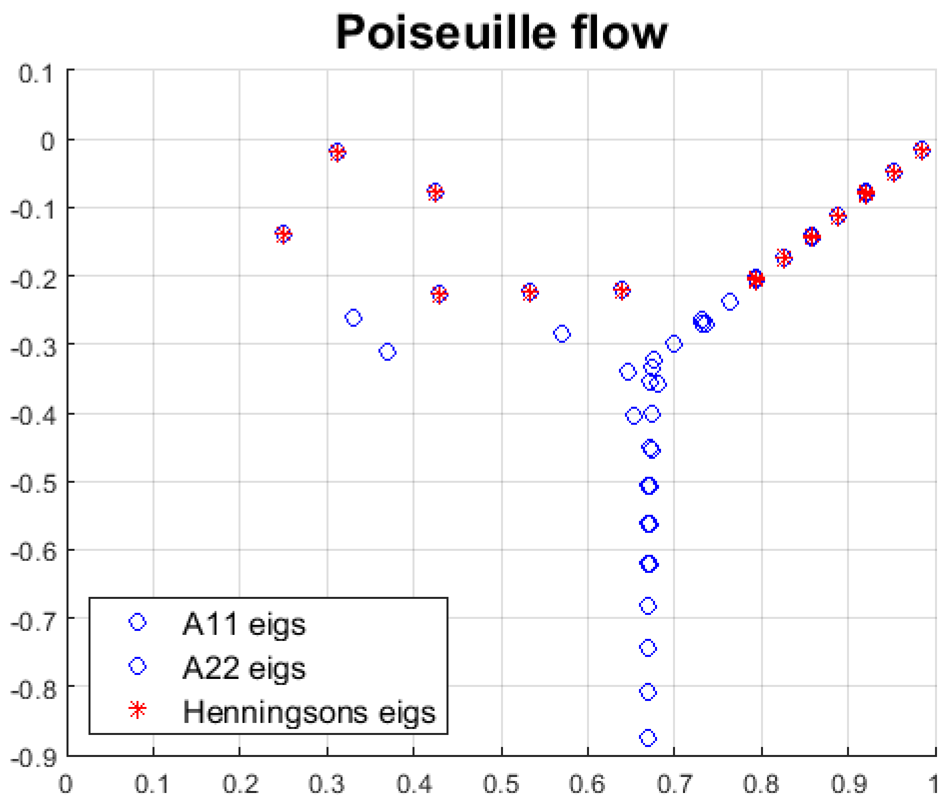

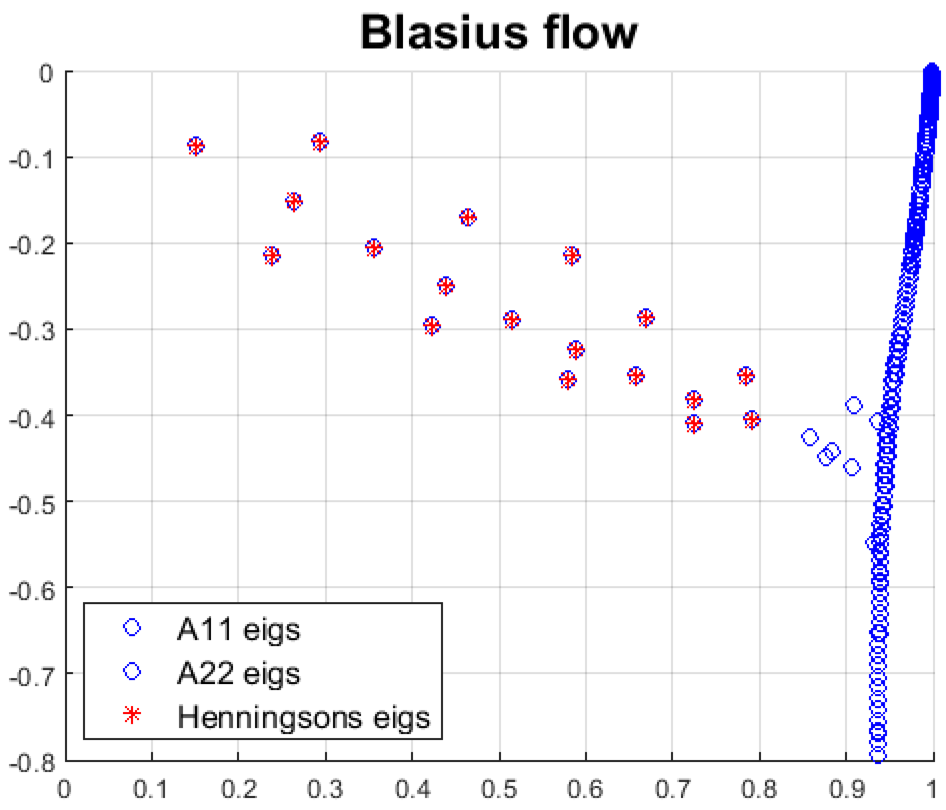

Navier-Stokes equations for perturbations

$$\partial_t \boldsymbol{u} = -U \cdot \nabla \boldsymbol{u} - \boldsymbol{u} \cdot \nabla \mathrm{U} - \nabla p + \frac{1}{Re} \nabla^2 \boldsymbol{u} - \underbrace{\boldsymbol{u} \cdot \nabla \boldsymbol{u}}_{\text{Nonlinear term}} + \boldsymbol{f}$$

- $\boldsymbol{f}$ – Forcing term (input)
- $\boldsymbol{u} = [u, v, w]^T$ – Velocity perturbation vector (output)
- U – Base flow (laminar solution)
- p – Pressure perturbation
- The nonlinear term can be rewritten as follows:

$$\boldsymbol{u} \cdot \nabla \boldsymbol{u} = \begin{bmatrix} u\partial_x u + v\partial_y u + w\partial_z u \\ u\partial_x v + v\partial_y v + w\partial_z v \\ u\partial_x w + v\partial_y w + w\partial_z w \end{bmatrix} = \underbrace{\begin{bmatrix} u & v & w & 0 & 0 & 0 & 0 & 0 & 0 \\ 0 & 0 & 0 & u & v & w & 0 & 0 & 0 \\ 0 & 0 & 0 & 0 & 0 & 0 & u & v & w \end{bmatrix}}_{\mathbf{u}_\Xi} \begin{bmatrix} \partial_x u \\ \partial_y u \\ \partial_z u \\ \partial_x v \\ \partial_y v \\ \partial_z v \\ \partial_x w \\ \partial_y w \\ \partial_z w \end{bmatrix}$$

Structure of $\mathbf{u}_\Xi$

$$\mathbf{u}_\Xi = \begin{bmatrix} u & v & w & 0 & 0 & 0 & 0 & 0 & 0 \\ 0 & 0 & 0 & u & v & w & 0 & 0 & 0 \\ 0 & 0 & 0 & 0 & 0 & 0 & u & v & w \end{bmatrix}$$

$$\bar{\sigma}(\mathbf{u}_\Xi) = \sqrt{\lambda_{\max}(\mathbf{u}_\Xi^T \mathbf{u}_\Xi)},$$

$$\mathbf{u}_\Xi^T \mathbf{u}_\Xi = \begin{bmatrix} u & 0 & 0 \\ v & 0 & 0 \\ w & 0 & 0 \\ 0 & u & 0 \\ 0 & v & 0 \\ 0 & w & 0 \\ 0 & 0 & u \\ 0 & 0 & v \\ 0 & 0 & w \end{bmatrix} \begin{bmatrix} u & v & w & 0 & 0 & 0 & 0 & 0 & 0 \\ 0 & 0 & 0 & u & v & w & 0 & 0 & 0 \\ 0 & 0 & 0 & 0 & 0 & 0 & u & v & w \end{bmatrix} = \begin{bmatrix} u^2 & uv & uw & 0 & 0 & 0 & 0 & 0 & 0 \\ uv & v^2 & vw & 0 & 0 & 0 & 0 & 0 & 0 \\ uw & vw & w^2 & 0 & 0 & 0 & 0 & 0 & 0 \\ 0 & 0 & 0 & u^2 & uv & uw & 0 & 0 & 0 \\ 0 & 0 & 0 & uv & v^2 & vw & 0 & 0 & 0 \\ 0 & 0 & 0 & uw & vw & w^2 & 0 & 0 & 0 \\ 0 & 0 & 0 & 0 & 0 & 0 & u^2 & uv & uw \\ 0 & 0 & 0 & 0 & 0 & 0 & uv & v^2 & uw \\ 0 & 0 & 0 & 0 & 0 & 0 & uw & vw & w^2 \end{bmatrix}$$

$$\bar{\sigma}(\mathbf{u}_\Xi) = \sqrt{u^2 + v^2 + w^2}$$

$$\|\mathbf{u}_\Xi\|_\infty = \sup_{y \in \mathcal{Y}} [\bar{\sigma}(\mathbf{u}_\Xi)] = \sup_{y \in \mathcal{Y}} \left(\sqrt{u^2 + v^2 + w^2} \right) = \sup_{y \in \mathcal{Y}} \|\boldsymbol{u}(y)\|_2$$

Approximating the structure of $\boldsymbol{\Delta}_{\mathbf{u}}$

- Repeated full – block matrix (Mushtaq, et al., 2024)

$$\boldsymbol{\Delta}_r = \{\mathbf{I}_{3\times 3} \otimes \Delta_r : \Delta_r \in \mathbb{C}^{3N_y \times N_y}\}$$

- Full – block matrix with different blocks (Liu and Gayme, 2021)

$$\boldsymbol{\Delta}_{nr} = \{\mathrm{diag}(\Delta_1, \Delta_2, \Delta_3) : \Delta_i \in \mathbb{C}^{3N_y \times N_y}, i \in \{1,2,3\}\}$$

- These imply the following relations between the sets:

$$\boldsymbol{\Delta}_{\mathbf{u}} \subset \boldsymbol{\Delta}_r \subset \boldsymbol{\Delta}_{nr} \subset \mathbb{C}^{3N_y \times N_y}$$

Solving the SSV **minimization problem** yields the following behavior:

$$\|\mathcal{H}_\nabla\|_{\mu_{\boldsymbol{\Delta}_{\mathbf{u}}}}^{-1}(k_x, k_z) \geq \|\mathcal{H}_\nabla\|_{\mu_{\boldsymbol{\Delta}_r}}^{-1}(k_x, k_z) \geq \|\mathcal{H}_\nabla\|_{\mu_{\boldsymbol{\Delta}_{nr}}}^{-1}(k_x, k_z) \geq \|\mathcal{H}_\nabla\|_\infty^{-1}(k_x, k_z)$$

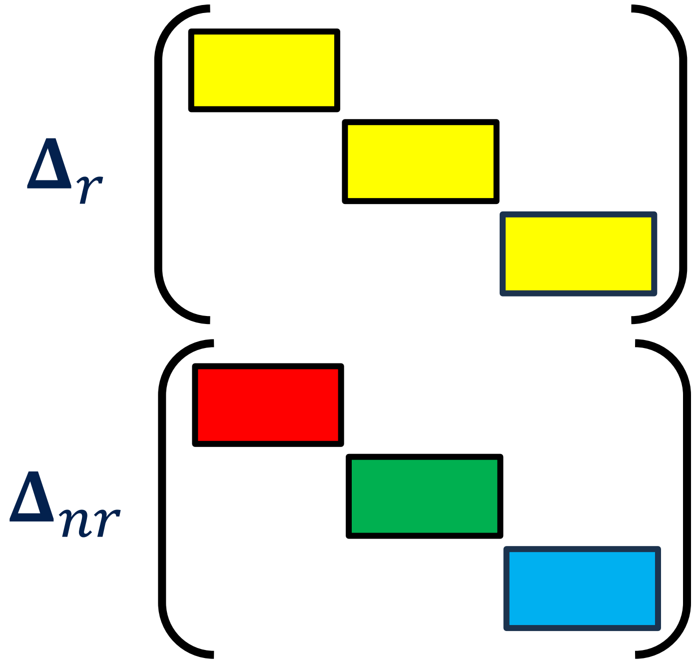

Optimization-Based Approach to Computing Amplification

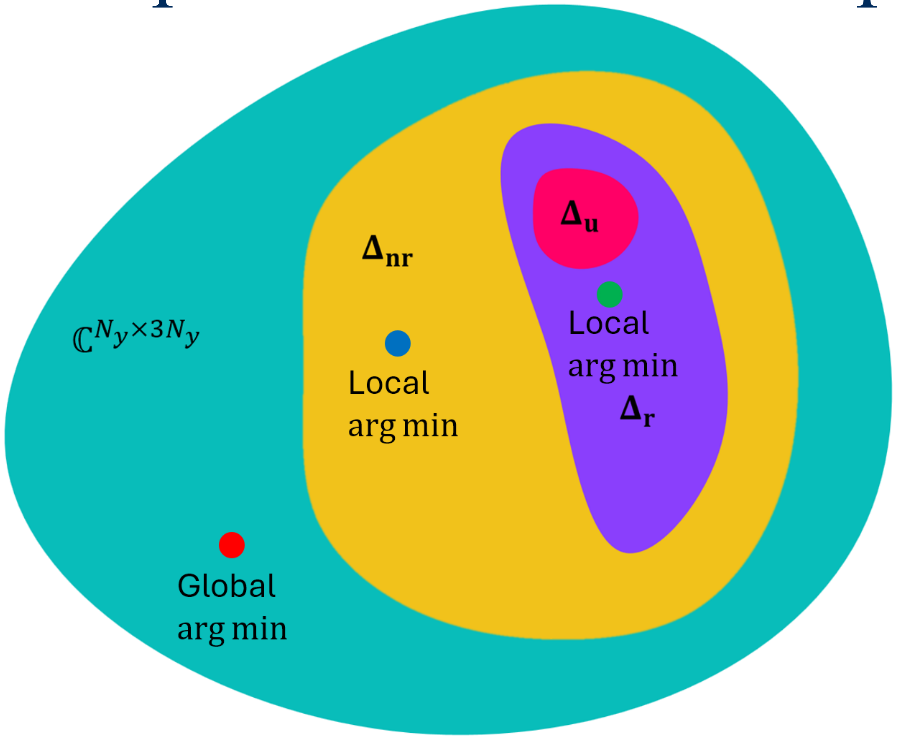

$$\mathbf{\Delta_u} \subset \boldsymbol{\Delta}_r \subset \boldsymbol{\Delta}_{nr} \subset \mathbb{C}^{N_y \times 3N_y}$$

$$\min_{\mathbf{u}_\Xi \in \mathbb{C}^{N_y \times 3N_y}} \bar{\sigma}(\mathbf{u}_\Xi) < \min_{\mathbf{u}_\Xi \in \boldsymbol{\Delta}_{nr}} \bar{\sigma}(\mathbf{u}_\Xi) < \min_{\mathbf{u}_\Xi \in \boldsymbol{\Delta}_r} \bar{\sigma}(\mathbf{u}_\Xi) < \min_{\mathbf{u}_\Xi \in \mathbf{\Delta_u}} \bar{\sigma}(\mathbf{u}_\Xi)$$

Results – Range of Reynolds Numbers (Blasius)

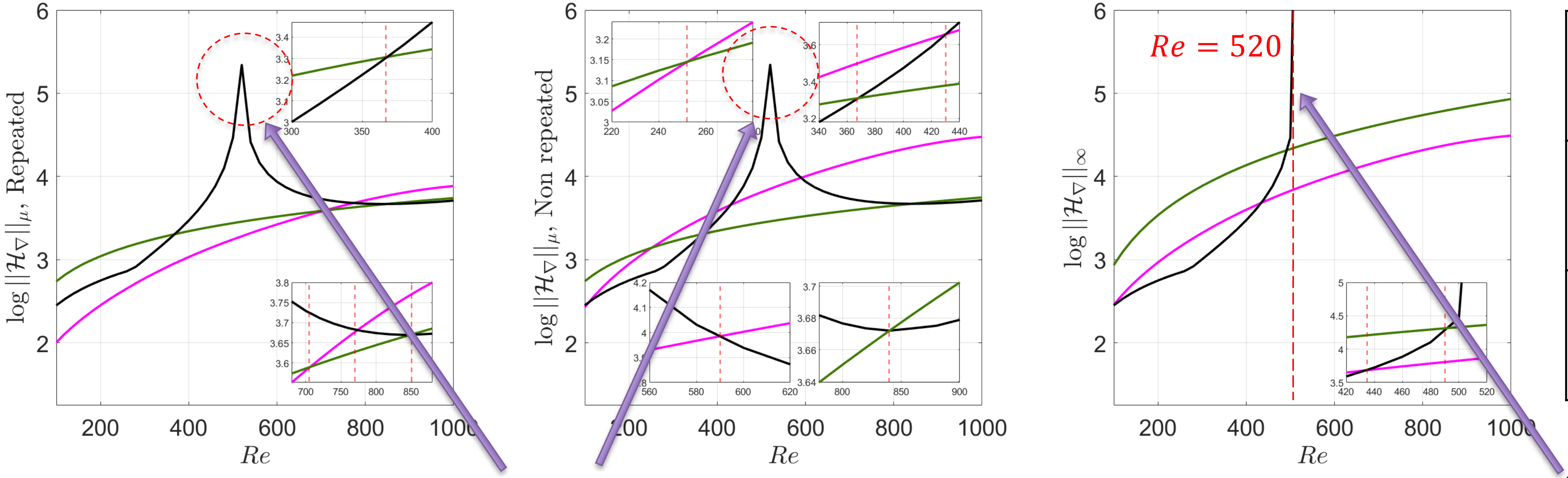

DLR (Dominant low Reynolds)

TS (Tollmien-Schlichting)

SPS (Spanwise periodic streaks)

Change of dominant mode

$\|\mathcal{H}_\nabla\|_\infty \to \infty$

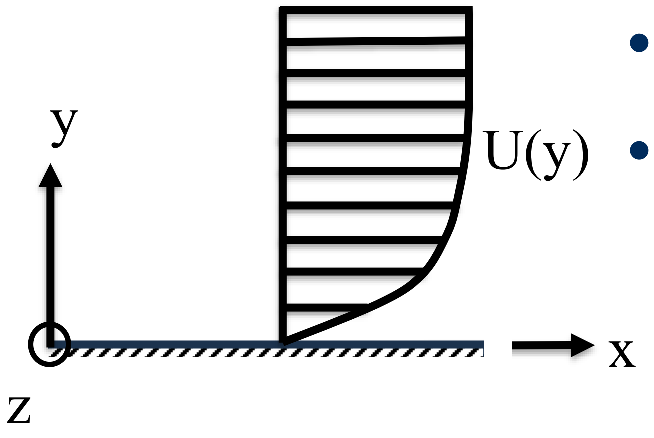

- Linear analysis predicts explosive growth at $Re \to 520$
- Nonlinear mechanisms cause a decay of the amplification of the TS mode - distributing energy between oblique modes

Results – Range of Reynolds Numbers (Poiseuille)

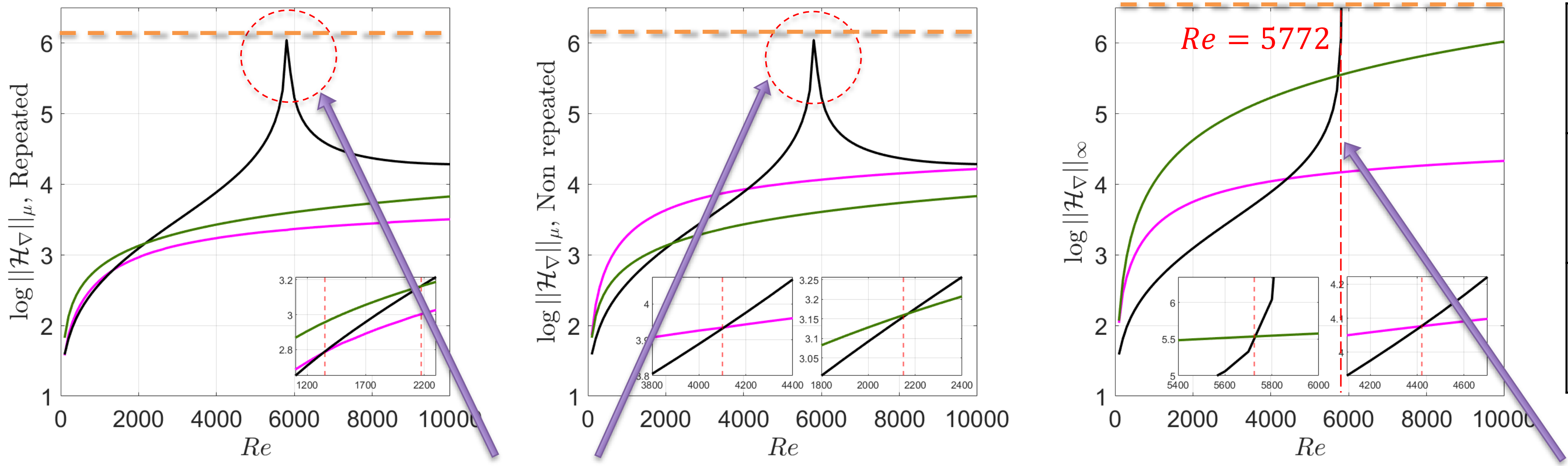

DLR (Dominant low Reynolds)

TS (Tollmien-Schlichting)

SPS (Spanwise periodic streaks)

Change of dominant mode

$\|\mathcal{H}_\nabla\|_\infty \to \infty$

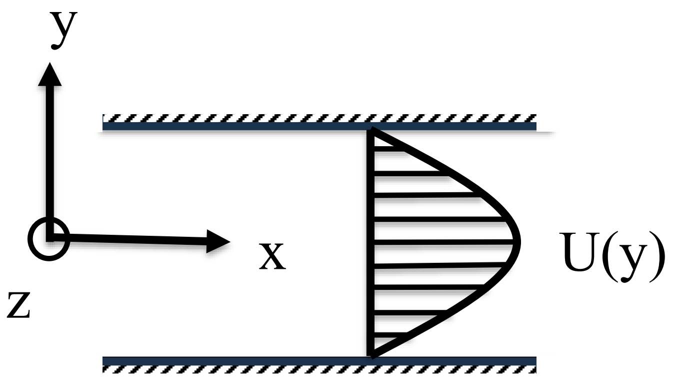

- Similar trends to Blasius case (at appropriate *Re*)
- All results comply with the hierarchical behavior:

$$\|\mathcal{H}_\nabla\|_{\mu_{\Delta_u}}(k_x,k_z) \le \|\mathcal{H}_\nabla\|_{\mu_{\Delta_r}}(k_x,k_z) \le \|\mathcal{H}_\nabla\|_{\mu_{\Delta_{nr}}}(k_x,k_z) \le \|\mathcal{H}_\nabla\|_\infty(k_x,k_z)$$

Stability for 3D modes

- Couette base flow
- Stability for perturbations of amplitude 10^{-3}
- 3D modes have both k_x and k_z components

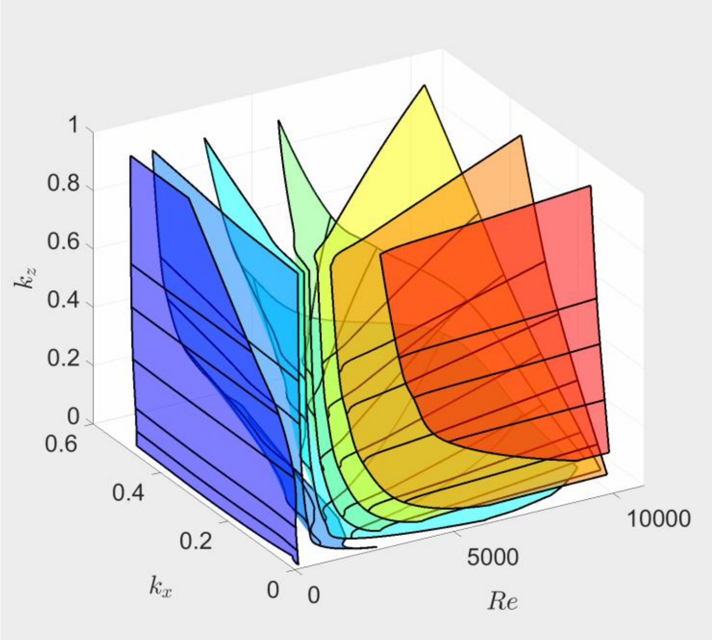

$\log_{10}(||\mathcal{H}_\nabla||_\infty^{-1})$ =-2.3 Isosurface
$\log_{10}(||\mathcal{H}_\nabla||_\infty^{-1})$ =-3.2 Isosurface
$\log_{10}(||\mathcal{H}_\nabla||_\infty^{-1})$ =-3.7 Isosurface
$\log_{10}(||\mathcal{H}_\nabla||_\infty^{-1})$ =-4 Isosurface
$\log_{10}(||\mathcal{H}_\nabla||_\infty^{-1})$ =-4.3 Isosurface
$\log_{10}(||\mathcal{H}_\nabla||_\infty^{-1})$ =-4.6 Isosurface
$\log_{10}(||\mathcal{H}_\nabla||_\infty^{-1})$ =-5.2 Isosurface

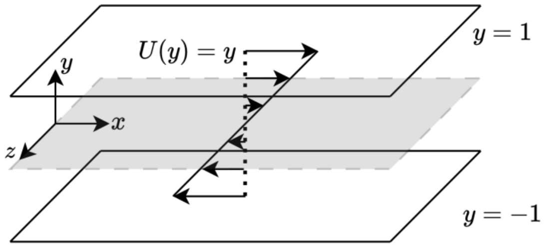

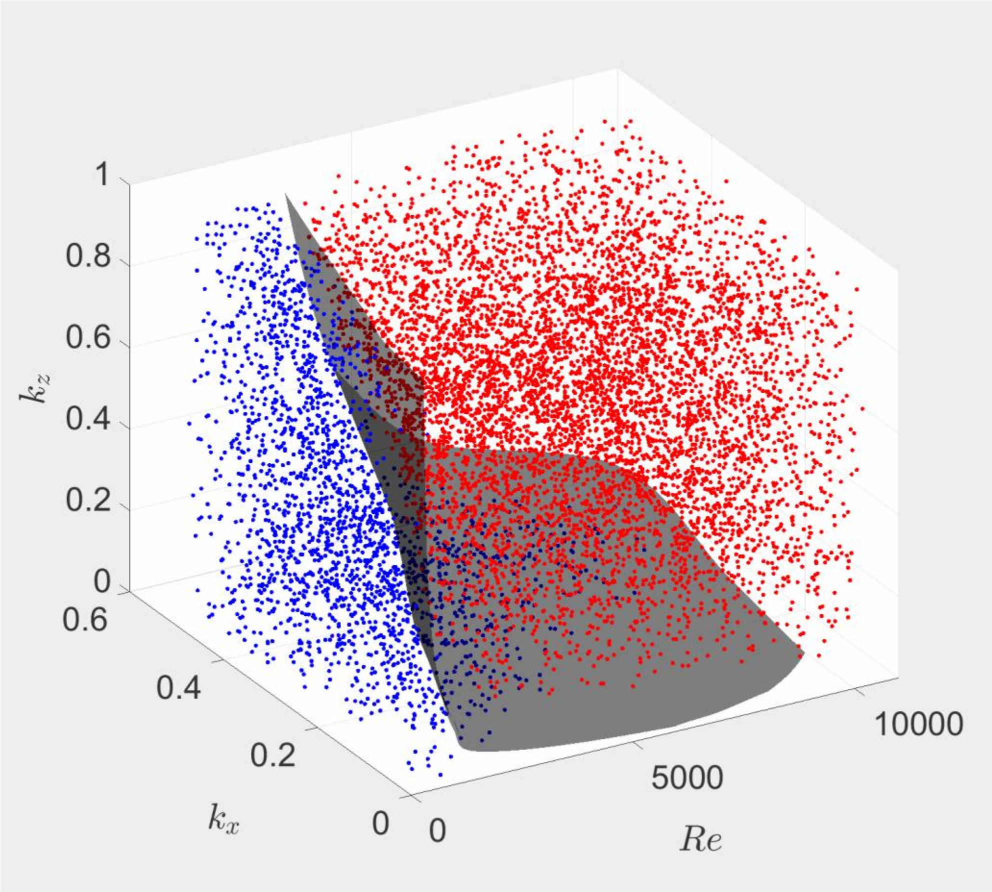

Stability for 3D modes

- Blasius base flow

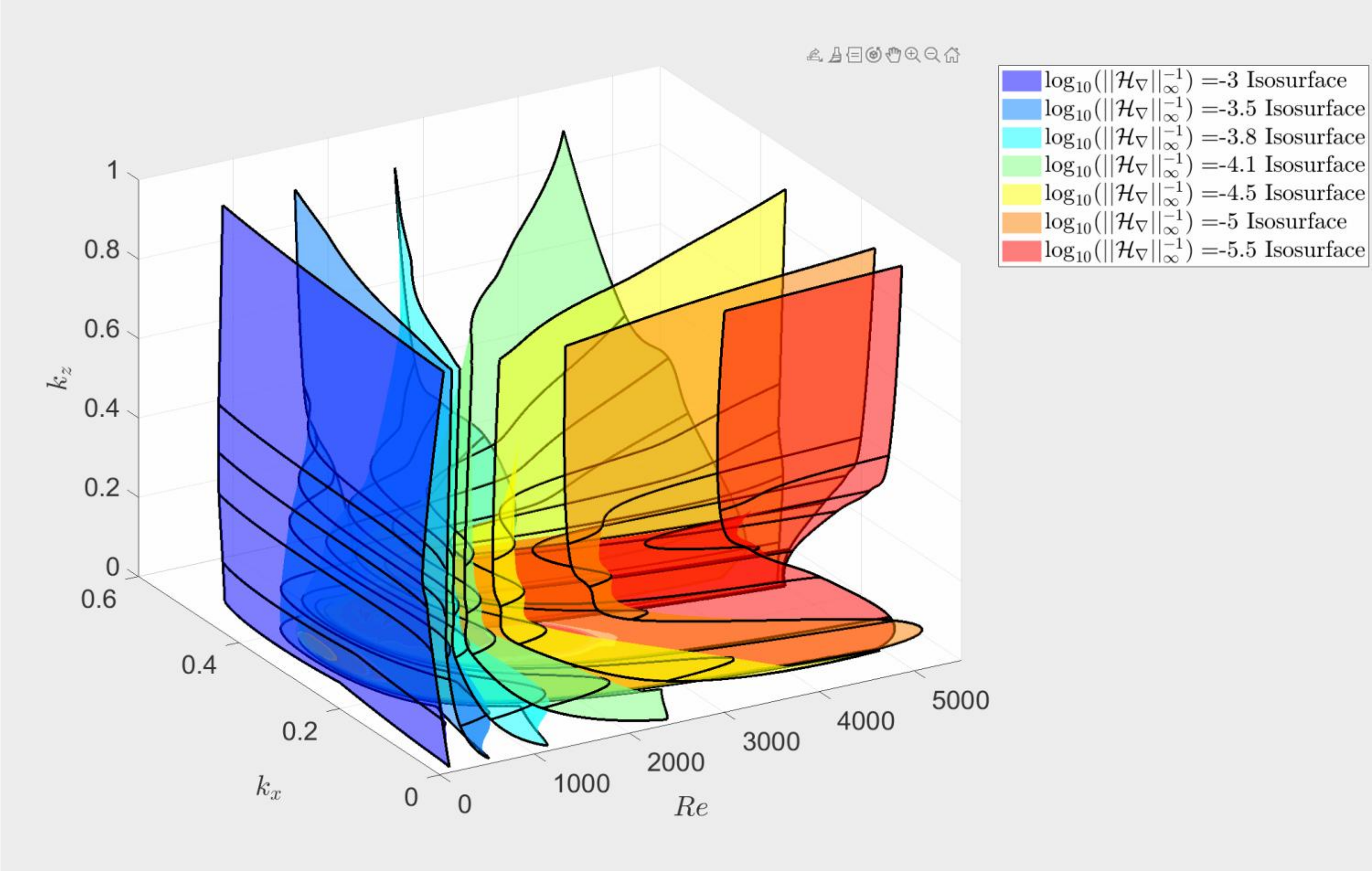

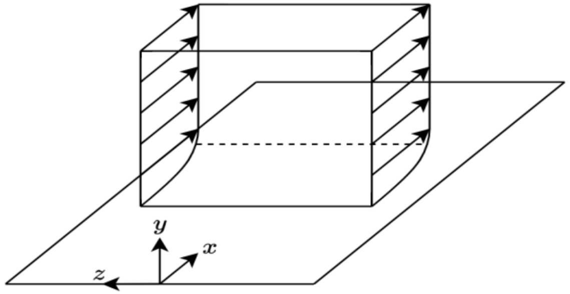

Generalized Power Iteration

Algorithm 3 Lower Bound: Generalized Power Iteration

(Initialization) Choose the number of iterations k_m and set $k = 0$. Select some unit-norm vectors $b^{[0]}, w^{[0]} \in \mathbb{C}^m$ and $a^{[0]} = z^{[0]} = 0 \in \mathbb{C}^m$.

while $k < k_m$ **do**

  (19a): $\beta := \|M b^{[k]}\|_2$ and $a^{[k+1]} := M b^{[k]}/\beta$.

  (19b): $z_L := \mathbf{Q}\left(L_{m_1}(a^{[k+1]}) L_{m_1}(w^{[k]})^{\mathrm{H}}\right) L_{m_1}(w^{[k]})$ and $z^{[k+1]} = L_{m_1}^{-1}(z_L)$

  (19c): $\beta := \|M^{\mathrm{H}} z^{[k+1]}\|_2$ and $w^{[k+1]} := M^{\mathrm{H}} z^{[k+1]}/\beta$.

  (19d): $b_L := \mathbf{Q}\left(L_{m_1}(w^{[k+1]}) L_{m_1}(a^{[k+1]})^{\mathrm{H}}\right) L_{m_1}(a^{[k+1]})$ and $b^{[k+1]} = L_{m_1}^{-1}(b_L)$.

  Set $k = k + 1$.

end while

Use $a^{[k_m]}$, $b^{[k_m]}$, $w^{[k_m]}$ and β to compute u, y and Δ.

Reprinted from Mushtaq, Bhattacharjee, Seiler, and Hemati, 2022.